Published in final edited form as:
Traffic. 2011 April ; 12(4): 483–498. doi:10.1111/j.1600-0854.2010.01155.x.

Basolateral sorting signals regulating tissue-specific polarity of heteromeric monocarboxylate transporters in epithelia

John J. Castorino[1], **Sylvie Deborde**[2], **Ami Deora**[2], **Ryan Schreiner**[2], **Shannon M. Gallagher-Colombo**[1], **Enrique Rodriguez-Boulan**[2], and **Nancy J. Philp**[1]

[1]Department of Pathology, Anatomy and Cell and Biology, Thomas Jefferson University, Philadelphia 19107

[2]Margaret M. Dyson Vision Research Institute, Weill Medical College of Cornell University, New York, NY 10021

Abstract

Many solute transporters are heterodimers comprised of non-glycosylated catalytic and glycosylated accessory subunits. These transporters are specifically polarized to the apical or basolateral membranes of epithelia but this polarity may vary to fulfill tissue-specific functions. To date, the mechanisms regulating the tissue-specific polarity of heteromeric transporters remain largely unknown. Here, we investigated the sorting signals that determine the polarity of three members of the proton-coupled monocarboxylate transporter (MCT) family, MCT1, MCT3 and MCT4, and their accessory subunit CD147. We show that MCT3 and MCT4 harbor strong redundant basolateral sorting signals (BLSS) in their C-terminal cytoplasmic tails that can direct fusion proteins with the apical marker p75 to the basolateral membrane. In contrast, MCT1 lacks a BLSS and its polarity is dictated by CD147, which contains a weak BLSS that can direct Tac, but not p75 to the basolateral membrane. Knockdown experiments in MDCK cells indicated that basolateral sorting of MCTs was clathrin-dependent but clathrin adaptor AP1B-independent. Our results explain the consistently basolateral localization of MCT3 and MCT4 and the variable localization of MCT1 in different epithelia. They introduce a new paradigm for the sorting of heterodimeric transporters in which a hierarchy of apical and basolateral sorting signals in the catalytic and/or accessory subunits regulates their tissue-specific polarity.

Keywords

basolateral sorting signal; monocarboxylate transporter; CD147; MDCK; retinal pigment epithelium

Introduction

Epithelial cells form selective barriers that regulate vectorial transport of water, ions, metabolites and nutrients between body compartments (1). An essential requirement for vectorial transport is the polarized distribution of transporter proteins and channels to apical and basolateral plasma membrane (PM) domains. During the past two decades, expression cloning has identified hundreds of apical and basolateral pumps, channels and transporters in epithelia. The polarity of these PM proteins in epithelia can vary in different tissues (2), however the mechanisms regulating targeting of these transporters to the correct PM domain in a tissue-specific fashion remain largely unknown.

Correspondence to N. J. Philp: Nancy.Philp@jefferson.edu or E. Rodriguez-Boulan: boulan@med.cornell.edu.

Studies with model monomeric PM proteins have elucidated their biogenic routes and many sorting mechanisms that regulate their polarized distribution in epithelial cells (3-4). Apical and basolateral PM proteins are synthesized in the endoplasmic reticulum (ER) and sorted in the trans-Golgi network (TGN) or in recycling endosomes (RE) into different carrier vesicles for delivery to their corresponding PM domains (3, 5). Recent studies have shown that the biosynthetic route of PM proteins often involves trafficking from Golgi to RE (3-5). Apical-basolateral sorting at the TGN and RE is mediated by sorting signals in the PM protein that are decoded by specific apical or basolateral trafficking machinery. Typically, apical sorting signals are complex and may be found in either the luminal, transmembrane, or cytoplasmic domains of the PM protein (4). In contrast, basolateral sorting signals (BLSS) are simple peptide sequences most often found within the cytoplasmic domain of the protein (3). Some BLSS resemble endocytic signals utilized during clathrin-mediated endocytosis, e.g. variations of the canonical endocytic YXXΦ, NPXY and dileucine motifs. Other basolateral signals are unrelated to endocytic signals, e.g. the tyrosine motifs in LDLR (6) and VSVG proteins (7), the GDNS motif of transferrin receptor (8-9), the multi-component basolateral signal of polymeric Ig receptor (10), the mono-leucine motifs found in CD147 (11) and stem cell factor (12), the EXEXΦΦ motif found in the M_3 muscarinic receptor (13), the PXXP motif in the epidermal growth factor receptor (14), and the PDZ-binding domain in syndecan-1 (15).

As expected from the similarity between endocytic signals and BLSS, clathrin is critically involved in the sorting of several single-span basolateral PM proteins from the TGN and recycling endosomes (16). Clathrin interacts with cargo proteins indirectly, via ~20 clathrin adaptors (17). Among these, the heterotetrameric adaptor AP1B is the only one to date known to participate in basolateral sorting (3, 18). AP1B localizes to recycling endosomes and sorts basolateral proteins in both biosynthetic and recycling routes (19-21). AP1B is expressed by most epithelia, but is not found in some specialized epithelia such as liver, retinal pigment epithelium (RPE) or the kidney proximal tubule (18, 22-23).

Many channels and transporters are not monomeric PM proteins but, rather, heterodimers composed of multi-span non-glycosylated catalytic α-subunits and single span glycosylated accessory β-subunits (24). Examples of these transporters include the Na-K ATPase and heteromeric amino acid and monocarboxylate transporters; they are all polarized to the basolateral PM in MDCK cells but their polarity varies *in vivo* depending on the particular epithelial tissue where they are expressed. Although considerable effort has been dedicated to elucidating the mechanisms responsible for Na-K ATPase localization, it is not yet clear to what extent its tissue-specific polarity is dictated by sorting signals in the catalytic or accessory subunit acting in concert with variations in the polarized trafficking machinery expressed by different epithelia (2). For other heterodimeric transporters, there is practically no information on the nature of the sorting mechanisms involved in their polarized distribution.

Here, we have studied the mechanisms responsible for tissue-specific polarity of the proton-coupled monocarboxylate transporters (MCTs). These are members of the SLC16 family of solute transporters, with twelve membrane spanning domains and both N- and C-terminal domains exposed to the cytoplasm (25). MCT isoforms have different tissue distributions and have been shown to transport an array of substrates including lactate and β-hydroxybutyrate (MCT1-4), amino acids (MCT10), and thyroid hormone (MCT8) (25-26). The coordinated activities of MCTs with other epithelial transporters are essential to facilitate lactate efflux from highly glycolytic epithelia (e.g. thyroid and small intestine) (27-29), as well as to facilitate the concentration-dependent transport of lactate from the subretinal space to the blood by the RPE that is essential for normal vision (30-31).

MCT1, MCT3, and MCT4 form a heterodimeric complex with CD147, a highly-glycosylated single-span type I transmembrane protein. The complex is assembled in the ER and the absence of either subunit results in degradation of the other one (32-34). Multiple MCTs are often coexpressed in a single epithelium; however, the polarity of the isoforms varies depending on the tissue. MCT1 (*SLC16A1*) is polarized to the basolateral membrane of intestinal and kidney epithelia (35-36), including the MDCK kidney epithelial cell line (32), but is apical in RPE (30-31) and epididymis (37). In contrast, MCT3 (*SLC16A8*) and MCT4 (*SLC16A3*) are localized basolaterally in all epithelia, including RPE (MCT3), thyroid (MCT4) (38), cultured RPE cells (MCT4) (33), small intestine (MCT4) (39) and MDCK cells (32). The sorting signals and machinery that regulate the variable localization of MCTs in different epithelia remain largely unknown.

Initial insight into the sorting of MCTs was provided by our identification of a BLSS in the cytoplasmic tail of CD147 consisting of a critical leucine (residue 252) (11). Mutation of this leucine to alanine in rat CD147 disrupted its basolateral distribution and resulted in localization of rCD147-L252A to the apical PM in MDCK cells. A very important observation was that overexpression of this apical mutant form of CD147 in MDCK cells, which express endogenously both MCT1 and MCT4 at the basolateral PM, redirected MCT1 but not MCT4, to the apical PM (32). Transfected MCT3 behaved similarly to MCT4 in that its basolateral localization was not disrupted by over-expression of rCD147-L252A. The distribution of MCTs in MDCK cells expressing the apical mutant form of CD147 mimics the distribution of these transporters in RPE cells (40). These experiments suggested the following working model (Figure 1): (i) MCT1 lacks a BLSS and relies on CD147 for its basolateral or apical localization, respectively in MDCK and RPE cells; (ii) MCT3 and MCT4 harbor strong BLSS that are dominant over sorting information in CD147 and determine their universal basolateral localization in MDCK, RPE, and other epithelial cell types (31-32, 37).

In the present studies we utilized two different experimental approaches to search for BLSS in MCT transporters. The first approach involved the expression of MCTs with truncations and mutations of their C-terminal domain in MDCK cells expressing rCD147-L252A. The second approach involved the expression of chimeric proteins consisting of extracellular and transmembrane domain of p75 neurotrophin receptor and different C-terminal tail domains of MCTs (41). It was previously shown p75 is expressed apically in MDCK cells, directed by O-glycans in its extracellular domain, but can be redirected to the basolateral PM by the addition of a cytoplasmic tail containing a BLSS (42-45). Our experiments identify and characterize novel and transportable BLSS in the C-terminal domains of MCT3 and MCT4 that determine their basolateral localization in both MDCK cells and RPE. They also demonstrate that the functional activity of these BLSS require clathrin, a key regulator of basolateral trafficking, and a clathrin adaptor other than AP1B. Finally, they also show that MCT1 lacks a BLSS and depends on CD147 for its apical/basolateral polarity. Since the BLSS of CD147 is functional in MDCK cells but not RPE cells (32), MCT1/CD147 heterodimers are basolaterally localized in MDCK cells but apically localized in RPE. The apical polarity of CD147 in RPE is likely determined by cryptic apical sorting information in its extracellular domain.

Thus, our experiments describe a new model to explain the variable polarity of heteromeric transporters in different epithelia. In this model, represented for MCTs in Figure 1, the polarity of a heteromeric transporter is guided by a hierarchy of BLSS and apical sorting signals in their transporting or accessory subunits. To successfully mediate basolateral localization, these signals require the presence of the appropriate basolateral sorting machinery in a given epithelium. This machinery is usually constituted by clathrin and clathrin adaptors, with variable expression in different epithelia.

Results

C-terminal cytoplasmic tails of MCT3 and MCT4 harbor BLSS

Examination of the primary sequence of the C-terminal tails of both MCT4 and MCT3 revealed that both had several acidic clusters, dihydrophobic motifs, single leucine residues, and C-terminal PDZ-binding motifs, which could function as BLSS (Figure S1A and S1B). The C-terminal cytoplasmic tail of MCT1 also contains elements that could function as BLSS, including a dileucine motif, acidic clusters and a PDZ-binding motif (Figure S1C).

To determine whether MCT4 and MCT3 have functional BLSS in their C-terminal cytoplasmic tails, our first approach was to stably express truncated forms of these proteins lacking their C-termini in an MDCK cell line stably overexpressing rCD147-L252A. As rationalized in Figure 1, if BLSS are present in their C-termini, the truncated MCT4 and MCT3 would be redirected to the apical PM by cryptic apical sorting signals in rCD147-L252A. We plated the cells on Transwell chambers and four days after reaching 100% confluency, we studied the surface polarity of MCTs by immunofluorescence and laser scanning confocal microscopy (LSCM). Strikingly, the truncated MCT4 and MCT3 were expressed preferentially on the apical surface (Figure 2A and B). The reversed apical polarity of these transporters strongly suggested that their C-terminal domains contain functional BLSS. In contrast, MCT1 is unlikely to contain BLSS as the full-length protein has an apical localization in MDCK cells expressing rCD147-L252A, as we previously reported (32).

To directly determine whether the C-termini of MCTs contain transportable BLSS or not, we utilized a second approach based on tagging these domains on the transmembrane and ecto-domains of an apical reporter, p75 (Figure 2C). This approach has the advantage of allowing the study of the presence or absence of basolateral sorting information in MCTs independently of their accessory subunit. We transfected the various p75:MCT-CT constructs into WT MDCK cells and studied their surface localization in non-clonal stable cell populations. Typically, four days after reaching confluence on Transwell chambers, the monolayers had transepithelial resistances of $175 \geq \Omega/cm^2$. The cells were either fixed and processed for LSCM or used for domain-selective cell-surface biotinylation (46). Confocal imaging showed that p75 localized to the apical membrane (Figure 2C1) while p75-MCT4:CT and p75-MCT3:CT localized to the basolateral membrane (Figure 2C2 and 2C3). Interestingly, the same result was observed after transfection of these constructs in human fetal RPE (hfRPE) cells (Figure S2). As these cells lack the clathrin adaptor AP1B; these results suggest that the BLSS in MCT4 and MCT3 do not require this adaptor to mediate basolateral localization. Additional experiments, described later, confirmed this hypothesis. Importantly, p75-MCT1:CT was localized to the apical membrane (Figure 2C4), supporting our hypothesis that MCT1 lacks intrinsic BLSS and depends on its accessory subunit CD147 for its polarized distribution.

Quantification of the steady-state polarity of the p75 fusion proteins by analysis of their colocalization with the endogenous basolateral MCT4 (Figure 2D) demonstrated strong colocalization in the case of p75-MCT4:CT (Pearson's colocalization coefficient 0.85) and p75-MCT3:CT (colocalization coefficient 0.65) and no colocalization in the case of apical p75 (colocalization coefficient −0.25) and p75-MCT1:CT (colocalization coefficient −0.11). Domain-selective cell-surface biotinylation experiments showed that 90% of p75-MCT4:CT was polarized to the basolateral membrane (Figure S3A). Given the strong agreement between biotinylation and quantitative analysis of confocal images, all subsequent polarity analyses were carried out using confocal colocalization analysis.

Since studies have suggested that mature lactate transporters are assembled through interactions between the ecto-domain of CD147 and the extracellular loops of MCTs (47), we expected that the p75-MCT4:CT protein would not interact with CD147. Indeed, co-immunoprecipitation studies in HEK-293 cells stably expressing p75-MCT4:CT showed that CD147 co-immunoprecipitated with MCT1 but not with p75-MCT4:CT (Figure S3B) demonstrating that p75 was a suitable reporter protein for studying CD147-independent MCT BLSS activity.

MCT4 has a BLSS that requires residues 431-441 of the C-terminal tail

To determine which of the potential BLSS was responsible for sorting MCT4 to the basolateral membrane, we stably expressed MCT4-GFP constructs with progressive truncations of the C-terminal tail into MDCK-rCD147-L252A cells. All of the MCT4 truncation fusion proteins were polarized to the basolateral PM of wild-type MDCK cells (data not shown). The fusion proteins with the more distal truncations, i.e. MCT4:G455Δ-GFP, MCT4:K448Δ-GFP, and MCT4:R441Δ-GFP, were all targeted to the basolateral membrane of MDCK cells coexpressing rCD147-L252A (Figure 3A). In contrast, the fusion proteins with the more proximal truncations, i.e. MCT4:K431Δ-GFP, MCT4:A424Δ-GFP, MCT4:Q418Δ-GFP, and MCT4:K413Δ-GFP, displayed a non-polarized localization in MDCK cells coexpressing rCD147-L252A (Figure 3A). The transition of polarity of the fusion proteins from exclusively basolateral to nonpolar suggested that the MCT4 BLSS contained elements that required amino acids 431 to 441. Additionally, truncation of the N-terminus of MCT4 did not disrupt basolateral expression of the fusion protein (Figure 3A5). The differences in polarity of the MCT4-GFP fusions were not the result of altered dependence on CD147 as all MCT4 truncation constructs required CD147 for expression at the PM as demonstrated by cell-surface biotinylation experiments following CD147 knockdown (Figure S4).

MCT4 has a bipartite BLSS

Based on the results from the MCT4 truncation studies, we next examined whether residues 409-441 of MCT4's cytoplasmic tail had basolateral sorting activity using the p75 reporter approach. We generated and stably expressed an array of p75-MCT4 C-terminal fusion proteins in MDCK cells and studied their steady-state distribution in polarized MDCK cells by immunofluorescence and LSCM. As shown in Figure 3B1, p75-MCT4:409-441 was sorted basolaterally, which is consistent with our findings with MCT4 truncation mutants described above. p75-MCT4:409-419 was sorted apically, indicating that the PXXP motif in this segment did not function as a BLSS (Figure 3B2). In contrast, p75-MCT4:423-441 was polarized to the basolateral membrane and co-localized with endogenous MCT4 (Figure 3B3). Examination of the region 423-441 indicated the presence of the acidic cluster $E_{425}E_{426}E_{427}$ upstream of two proline residues. Several BLSS contain acidic clusters, e.g. those in M_3 muscarinic receptor, the receptor tyrosine kinase ErbB2, or proline motifs, e.g. those of ErbB2, EGFR, and the multifunctional matrix metalloproteinase and receptor protein ADAM10. Hence, we further analyzed the 423-441 segment by determining the localization of two fusion proteins, p75-MCT4:424-431, containing the acidic cluster, and p75-MCT4:432-441, containing the di-proline motif. Both fusion proteins were polarized to the apical membrane of MDCK cells (Figure 3A4 and 3A5) indicating that elements from both 424-431 and 432-441 are required for BLSS activity. Quantitative analysis of the polarity of these fusion proteins is shown in Figure 3C.

To confirm that both the acidic and di-proline motifs were required for BLSS activity, we generated p75:MCT4:423-441 constructs with either all three glutamate residues mutated to alanine (p75-MCT4:423-441:EEE-AAA) or with both proline residues mutated to alanine (p75-MCT4:423-441:PP-AA). As shown in Figure 4A, mutation of either the glutamate or

proline residues to alanine resulted in apical sorting of the fusion proteins, demonstrating that both of these motifs are required for BLSS activity. Additional mutagenesis of the individual acidic residues demonstrated that both E425 and E427 were essential for BLSS activity (Figure 4B1 and 4B3). Mutation of E426 led to a non-polar expression pattern indicating some disruption of BLSS activity. Interestingly, individual mutation of residues P432 or P433 to alanine did not disrupt basolateral expression of the fusion protein (Figure 4C), demonstrating that the presence of a single proline was sufficient for BLSS activity. However, mutation of individual proline residues promoted intracellular accumulation of the fusion proteins (more easily observed in the X-Y projections; Figure S5), suggesting that although basolateral polarity was preserved, trafficking to the cell surface, recycling, or degradation of these fusion proteins was impaired.

MCT4 has a second BLSS in residues 441-465 of the C-terminal tail

In order to determine whether the acidic and di-proline motifs functioned as BLSS in the context of the full-length protein, a MCT4-GFP fusion construct was generated with E425, E426, E427, P432, and P433 all mutated to alanines. Surprisingly, this fusion protein was restricted to the basolateral membrane in MDCK-rCD147-L252A cells (Figure 5A1). However, when the same mutations were introduced into MCT4 truncated at R441 (MCT4:R441Δ-GFP), the fusion protein was nonpolar in MDCK-rCD147-L252A cells (Figure 5A2) indicating that the BLSS had been disrupted.

While these experiments confirmed that the acidic and proline motifs functioned as part of a BLSS, they also suggested the presence of an additional BLSS in the most distal region (residues 441-465) of MCT4's cytoplasmic tail. This was not apparent in the progressive truncation mutants as removal of the distal BLSS was not sufficient to disrupt the polarity of MCT4 since the proximal BLSS was present. To test for basolateral sorting activity in the residues 441-465, a p75-MCT4:441-465 construct was generated and stably expressed in MDCK cells. As shown in Figure 5B1, p75-MCT4:441-465 was restricted to the basolateral membrane of MDCK cells where it co-localized with the endogenous MCT1. This region contains two potential EXEXΦΦ motifs and a C-terminal type-I PDZ-binding motif (ETSV) that could function as BLSS. Mutation of residues E442, E444, F446, L447, E450, E452, V457, and V458 to alanine in p75-MCT4:441-465 (Figure 5B2) or deletion of the C-terminal PDZ-binding motif in p75-MCT4:441-460 (Figure 5B3) resulted in partial disruption of polarity of the reporters. These findings suggest that both domains contribute to basolateral sorting of MCT4.

MCT3 has two BLSS in its C-terminal tail

To identify and characterize the BLSS of MCT3, we used a fusion construct containing the ecto and TM domains of p75 and different domains of the C-terminal tail of MCT3. Fusion proteins containing either the juxtamembrane region (p75-MCT3:432-450, Figure 6A1) or the most distal region (p75-MCT3:485-504, Figure 6A3) of MCT3's C-terminal tail were targeted apically whereas p75-MCT3:451-484 was targeted basolaterally (Figure 6A2). These experiments indicated that MCT3's BLSS was localized in the central domain of its C-terminal tail and that the type-III PDZ-binding domain at its C-terminal end did not have BLSS activity.

In order to more precisely define the BLSS of MCT3, we analyzed the basolateral sorting activity of two smaller fragments within residues 451-484. Fusion proteins containing either of these elements (p75-MCT3:451-469 and p75-MCT3:470-484) were both targeted basolaterally in polarized MDCK (Figures 6B1 and 6C1) and hfRPE cells (Figure S2C and S2D). Further mutational analysis was performed on each of these regions to pinpoint the BLSS. Within the 451-469 region, mutation of the upstream acidic residues

(MCT3:451-469:DEDE-AAAA, Figure 6B2) or removal of the hydrophobic amino acids and prolines (MCT3:451-464, Figure 6B3) led to apical expression of the p75 fusion proteins. Within the 470-484 region, mutation of residues E471 and E472 to alanines (MCT3:470-484:EE-AA) led to nonpolar expression of the fusion protein (Figure 6C2) while mutation of the dihydrophobic motif to alanines (MCT3:470-484:VL-AA) led to apical expression of the reporter fusion (Figure 6C3). These experiments indicate that MCT3 has two redundant BLSS, constituted by acidic amino acids followed by either proline or hydrophobic residues. Colocalization analysis of confocal images confirmed polarity of p75-MCT3 fusion proteins (Figure 6D).

The BLSS of MCT3 and MCT4 are transferable to MCT1

Our previous studies suggested that MCT1 lacks a BLSS as evidenced by colocalization with CD147 in the apical membrane of RPE (40) and with rCD147-L252A in MDCK cells (32). In the current studies, p75-MCT1:CT was polarized to the apical membrane of MDCK cells thereby confirming the lack of a BLSS in the C-terminal tail of MCT1 (Figure 2C4). When MCT1-GFP was stably coexpressed with rCD147-L252A in MDCK cells, MCT1-GFP was redirected to the apical membrane (Figure 7A). To determine whether the BLSS of MCT3 and MCT4, identified in this report, could confer dominant basolateral sorting activity to MCT1, we constructed GFP fusion proteins comprised of MCT1 with the C-terminal domains of MCT3 or MCT4 appended to its C-terminal tail. These fusion proteins were localized basolaterally in both wild-type MDCK cells (not shown) and in MDCK cells overexpressing rCD147-L252A (Figure 7B and 7C). Thus, the BLSS of MCT3 and MCT4 are transferable.

Basolateral sorting of MCTs in MDCK cells is clathrin-dependent, but AP1B-independent

We have recently shown that many BLSS, including that of CD147, are decoded by a basolateral sorting mechanism that requires the coat protein clathrin (16). To determine whether the basolateral sorting of MCT4 is clathrin-dependent, we studied the distribution of endogenous MCT4 and of transfected p75-MCT4:CT in MDCK cells following knock down of clathrin heavy chain (CHC) generated as we recently reported (16). Domain-selective cell-surface biotinylation of MDCK cells transfected with control and CHC-specific siRNA showed that CHC silencing increased apical expression of MCT1, MCT4 and p75-MCT4 by at least 50% while the polarity of the basolateral marker Na-K ATPase and the apical marker GP135 were altered only slightly (Figure 8A). Immunofluorescence LSCM confirmed loss of polarity of p75-MCT4, MCT1, and MCT4 in CHC siRNA-treated cells (Figure 8B). Among the clathrin adaptors, only AP1B has been identified as a regulator of basolateral sorting (see Introduction). Experiments described above indicated that MCT3 and MCT4 are localized basolaterally in RPE cells (Figure S2), which do not express AP1B, suggesting that their BLSS do not mediate basolateral localization via this adaptor. To further investigate this point, we studied the expression of endogenous MCT4 and MCT1 in MDCK cells stably knocked-down of the AP1B complex component μ1B (20). Analysis of these cells by immunofluorescence and LSCM indicated that both MCT1 and MCT4 were basolaterally expressed (Figure 8C), confirming that these transporters do not require AP1B for their basolateral localization. Further evidence for the AP1B-independent sorting of MCT1 was provided by immunofluorescence labeling of cryosections of mouse kidney and retina with a MCT1 antibody. These experiments showed that MCT1 is polarized to the basolateral PM in proximal convoluted tubule (PCT) and to the apical PM in the RPE (Figure 8D and 8E). Since neither PCT nor RPE express AP1B (22-23), these experiments demonstrate that *in vivo*, as previously shown *in vitro*, basolateral sorting of MCT1 is AP1B-independent.

The BLSS of MCT3 and MCT4 are stronger than the BLSS of CD147

As shown above, fusion proteins consisting of the extracellular and transmembrane domains of p75 and C-terminal cytoplasmic tails of MCT4 or MCT3 were trafficked to the basolateral membrane in MDCK cells. We have previously shown that the C-terminal domain of rCD147, when appended to the extracellular and transmembrane domains of Tac (the interleukin-2 receptor α-subunit), directed the fusion protein to the basolateral PM of MDCK cells (11)(Figure 9A). Surprisingly, a fusion protein with the C-terminal tail of rCD147 appended to p75 (p75-rCD147:CT) was expressed apically in MDCK cells (Figure 9B). The apical polarity of p75-rCD147:CT and the basolateral polarity of Tac-rCD147:CT in MDCK cells demonstrates that not all BLSS are universally dominant over apical sorting signals, and that their ability to target a given protein to the basolateral PM depends on their strength relative to apical sorting information in the ectodomain, as shown by CD147's BLSS. These observations provide useful insights on the mechanisms regulating the polarity of these transporters in different epithelia.

Discussion

In the current study, we systematically investigated the mechanisms regulating isoform-specific trafficking of heteromeric monocarboxylate transporters. Trafficking of heteromeric transporters is a complex problem, typified by the field of Na-K ATPase sorting, where, in spite of many years of study, the sorting signals involved remain controversial. In contrast, our previous (32) and current studies with MCTs, provide the first clear picture of the complementary roles of the catalytic and accessory subunits in the sorting of a family of heteromeric transporters.

We report here that MCT3 and MCT4, the low affinity transporters which facilitate lactate efflux from various types of cells, have redundant bipartite BLSS in their C-terminal cytoplasmic tails. In contrast, MCT1, a high affinity transporter that can move lactate into or out of cells depending on metabolic needs, lacks a BLSS. The variable polarity of MCT1 in different tissues is dictated by its accessory subunit CD147, which has a BLSS in its C-terminal cytoplasmic tail that is functional in MDCK cells but not in RPE (further discussed below). CD147 appears to have cryptic apical information in its ectodomain that, when its BLSS is mutated, directs it to the apical surface, bringing MCT1 along (32). Taken together, our experiments support a model for the polarized sorting represented in Figure 1. According to this model, the strong BLSS in MCT3 and MCT4 guarantee their basolateral localization in multiple epithelia. In contrast, the combination of no BLSS in MCT1 with a weak BLSS in CD147, variably recognized by different epithelia, allows for a flexible localization of the MCT1/CD147 heterodimer in different epithelia, adapted to their specific physiologic requirements for lactate transport.

To identify the BLSS in MCT4, we used two complementary approaches: coexpression of MCT4 C-terminal truncation constructs with rCD147-L252A in MDCK cells and expression of p75-MCT C-terminal tail chimeric proteins MDCK cells (Figure 1). Our studies with the first experimental approach indicated that although both N- and C-terminal tails of MCT4 are cytoplasmic, only the C-terminal tail harbors BLSS (Figure 3). Truncation of the C-terminal tail of MCT4 altered sorting but did not disrupt the dependence on CD147 for trafficking to the PM (Figure S4), indicating that the interaction between the two molecules occurs at the level of the transmembrane or ecto domains, which is consistent with the findings of others (47-48). The C-terminal tail of MCT4 is highly conserved across species and contains a number of different elements that could dictate BLSS activity, e.g., a PXXP motif, an EXEXΦΦ, leucine, proline, and acidic residues, and a PDZ-binding domain. Our experiments narrowed down one BLSS of MCT4 to a 19 amino acid sequence A_{423}AEEEKLHKPPADSGVDLR$_{441}$. The critical residues within this sequence were

identified as E425, E427 and either P432 or P433. The core EE and PP functional elements were very well conserved across all listed mammalian MCT4 orthologs and at least EE and one P were conserved across all vertebrate species examined (Figure S1A). At first glance, these BLSS appear to be unlike any reported previously; however, on more careful inspection, elements of these signals share features of sorting motifs identified in other transmembrane proteins. Prolines have been reported to be critical amino acids of the BLSS of ErbB2, ADAM10, and EGFR (14, 42, 44, 49). Acidic residues have been shown to be necessary for basolateral sorting of GAT-2, the M_3 muscarinic receptor, ErbB2, Aquaporin 4, and Furin (42, 44, 50-51). Interestingly, other proteins have acidic residues in close proximity to critical residues of the BLSS, including TGFβ-R and EGFR (14, 52).

In our effort to confirm that this BLSS was functional in the full-length protein, we mutated the critical residues of the BLSS in full-length MCT4-GFP and coexpressed it with rCD147-L252A in MDCK cells. To our surprise, the mutant MCT4 was restricted to the basolateral membrane, which suggested to us that additional basolateral sorting information was present in the distal 25 amino acids of the C-terminal tail of MCT4. Indeed, subsequent studies showed that p75-MCT4:441-465, which contains two EXEXΦΦ motifs and a type-I PDZ-binding domain, was targeted to the basolateral membrane in MDCK cells. Additional experiments suggested that the basolateral sorting activity was present in the both the highly conserved acidic and hydrophobic residues and the type-I PDZ binding domain (Figure 5B). While there are no reports in the literature of type-I PDZ-binding domains acting as BLSS, it is possible that PDZ-binding motif-mediated BLSS activity was masked by more proximal BLSS in these proteins as we discovered with MCT4. The type-II PDZ-binding domain of syndecan-1 functions as BLSS (15).

We also utilized the p75 reporter approach to search for the BLSS of MCT3. This approach identified two independent BLSS in the C-terminal tail of MCT3: A_{451}SDTEDAEAEGDSEPLPVV$_{469}$ and A_{470}EEPGNLEALEVLSA$_{484}$. Mutational analysis of these regions indicated that the core BLSS were composed of acidic clusters followed by proline or hydrophobic residues. Dihydrophobic motifs are found within the BLSS of the M_3 muscarinic receptor, MICA, Furin, and NBC1 (13, 51, 53-54). Additionally, while the C-terminal cytoplasmic tail of MCT3 is not as highly conserved among mammals as MCT4, all mammalian species examined do contain an acidic cluster followed by at least one hydrophobic residue and proline within the region that would correspond to human residues 451-469. The EE and VL motifs of the second MCT3 BLSS (within 470-484) are also well conserved among mammalian species (Figure S1B). Interestingly, in the context of a p75 fusion protein, the type-III PDZ-binding domain at the C-terminus of MCT3 did not exhibit dominant basolateral sorting activity (Figure 7).

The C-terminal cytoplasmic tail of MCT1 contains elements found in the MCT4 and MCT3 BLSS including two acidic clusters and dileucine residues (Figure S1C), however this region does not have detectable BLSS activity when appended to the cytoplasmic domain of p75 (Figure 2C). In the MCT1 C-terminal tail, the acidic clusters are not 4-6 residues upstream of dihydrophobic motifs (or prolines) indicating that the particular spacing of the elements is required for MCT4 and MCT3 BLSS activity.

The tissue-specific distribution of PM proteins in different epithelia is determined by their sorting signals in combination with the particular sorting machinery expressed by a given epithelium. We recently reported that clathrin is a key regulator of basolateral trafficking and that CD147 is sorted basolaterally by a clathrin-dependent mechanism (16); however, these studies did not address whether the clathrin dependency of CD147 is determined by its own BLSS or by BLSS in the MCT transporters.

Here we report that clathrin knock-down in MDCK cells results in depolarization of p75-MCT4 and endogenous MCT4 (Figure 8), indicating that the strong BLSS we have discovered in its C-terminal tail requires interaction with clathrin adaptors to mediate basolateral localization. We do not know yet whether clathrin is involved in the basolateral sorting of MCT3. However, it is clear that the well characterized clathrin adaptor AP1B is not involved in the basolateral sorting of either MCT3 or MCT4, because of the following evidence: (i) MCT3 and MCT4 are basolateral in RPE cells (Figure S2) (33), which do not express AP1B (22) and (ii) MCT4 is expressed basolaterally in MDCK cells knocked-down of AP1B (Figure 8c). The BLSS we have described in these transporters are the first AP1B-independent BLSS described to date. They constitute useful tools for identifying the alternative clathrin adaptors involved in their basolateral localization.

Unlike MCT3 and MCT4, MCT1 shows a variable polarity in different epithelia. It is polarized to the basolateral membrane in epithelia lining the colon, proximal convoluted tubule and MDCK cells but is polarized apically in the RPE and the epididymis. We found that MCT1 was depolarized by clathrin knock-down and not by AP1B knock-down in MDCK cells (Figure 8). These experiments indicate that the BLSS of CD147 is not recognized by AP1B and, hence, that the absence of AP1B in RPE cells does not account for the apical localization of MCT1 in this epithelium. This conclusion is further strengthened by the observation that MCT1 is basolaterally localized in the proximal convoluted tubule of the kidney, which we have recently shown lacks AP1B (23). As the polarity of MCT1 is determined by its accessory protein CD147, future experiments must address what clathrin adaptors are involved in the basolateral sorting of this protein. An apical reporter approach such as reported in this paper may provide the best chance to identify this adaptor.

An important conclusion from this study and from our previous work (11) is that CD147, deprived of its BLSS, is sorted apically in MDCK cells and is capable of redistributing MCT1 to the apical membrane. Furthermore, MCT1 is sorted apically in RPE cells, which cannot recognize the BLSS of CD147 and is likely responsible for the apical distribution of MCT1 in this epithelium (Figure 1). Taken together, these observations suggest that, to mediate basolateral localization of CD147, its BLSS must overcome cryptic apical sorting information in CD147. Indeed, we have previously reported that the C-terminal cytoplasmic tail of CD147 can redirect the apical reporter Tac to the basolateral PM in MDCK cells (11). In contrast, we report here that the BLSS of CD147 cannot redirect the apical reporter protein p75 to the basolateral PM in MDCK cells, as the p75-rCD147:CT chimera was trafficked to the apical membrane. Similarly, the BLSS of the ATP receptor $P2Y_1$ is unable to redirect p75 to the basolateral membrane (55). On the other hand, we also report here that the BLSS of MCT3 and MCT4 are potent enough to redirect p75 to the basolateral PM. The most parsimonious conclusions suggested by these experiments are: (i) BLSS of CD147 is weaker than those found in MCT3 and MCT4 (ii) the differential strength of these signals may play an important role in accounting for the consistent basolateral localization of MCT3 and MCT4 for the variable localization of MCT1 in different epithelia.

What is the nature of the apical sorting signal in CD147 responsible for targeting this protein apically in RPE cells or in MDCK cells when its BLSS is deleted (11)? CD147 is a highly-glycosylated transmembrane protein and both N- and O- glycans have been posited to act as apical sorting signals (4). p75 contains a variety of apical targeting signals, including O-glycans and N-glycans; one or more of these signals might be dominant over CD147's BLSS. Recent work in the controversial field of Na-K ATPase sorting suggests that glycosylation of its beta subunit might contribute to its apical localiization in some specialized epithelia, e.g RPE and epididymis (56), reviewed by Philp et al.(2). As the expression of glycosyltransferases is variable in different tissues (57-60) and CD147 is a

highly-glycosylated protein, our findings support the hypothesis that variable glycosylation may play a role in the variable polarity of MCT1/CD147 in different epithelia.

In summary, our results provide new insights into the mechanisms that mediate the localization of MCTs in different epithelia. They suggest that the flexible polarity of heteromeric transporters in various epithelia is determined by a combination of sorting signals in the non-glycosylated catalytic subunit and the highly-glycosylated accessory subunit. MCT3 and MCT4 harbor strong redundant BLSS that are transferable and dominate over apical sorting information in CD147. MCT1 has no BLSS and therefore its trafficking is dependent on whether the apical or basolateral sorting signal of CD147 is dominant in a given epithelium. Future studies will search for clathrin adaptors involved in the recognition of the BLSS of MCTs and CD147 and investigate the intracellular routes followed by these adaptors in the various epithelial cell types where they are expressed.

Materials and Methods

Generation of Expression Vectors

MCT4, MCT3, and MCT1 PCR products were amplified from cDNA prepared with total RNA extracted from MDA-MB-231 or hfRPE cells as previously described (61). Forward primers included optimized Kozak consensus sequences. Primers used to generate the various deletion constructs are listed in Table S1. PCR products were digested with XhoI and BamHI and cloned into these sites of the pEGFP-N1 vector (BD Biosciences) to generate GFP-fusion expression constructs.

In order to more easily attain lines of MDCK cells expressing both the MCT4-GFP fusions and rCD147-L252A, the rCD147-L252A generated previously was excised from the pcDNA3.1 vector backbone with EcoRI and XhoI and ligated into pcDNA6/V5-His A (Invitrogen) in order to obtain a blasticidin-resistant rCD147-L252A expression construct.

p75 encoding the extracellular and transmembrane domains were amplified by PCR with primers 5′-agtcagatctgccaccatgggggcaggtgccac-3′ and 5′-agctgcggccgcggcgcgcctcattctgttagtggggtggtctggatcccgctgttccacctcttgaaggc-3′ which included 5′-BglII, 3′-internal BamHI and AscI sites, and a 3′-NotI site. The coding insert was digested with BglII and NotI and ligated into these sites of the pEGFP-N1 vector, resulting in a construct with a CMV promoter and SV40 3′ untranslated region while removing the EGFP open reading frame. The resulting vector was named pCMV p75. Depending upon the region of the MCT to be inserted in the pCMV p75 vector, either the region was amplified by PCR and digested or oligonucleotides containing 5′ BamHI and 3′ AscI sticky ends were synthesized, annealed, and phosphorylated before ligating into these sites of pCMV p75. Oligonucleotides utilized for these constructs are shown in Table S2.

Mutation of E425, E426, and E427 to alanine were performed by site-directed mutagenesis with a Quick Change II mutagenesis kit (Stratagene) using the primer pair 5′-gtggcggccgcggcggcggcgaagctccacaag-3′ and 5′-cttgtggagcttcgccgccgccgcggccgccac-3′. Mutations of P432 and P433 to alanine were performed with the primer pair 5′-gaagctccacaaggctgctgcagactcggg-3′ and 5′-cccgagtctgcagcagccttgtggagcttc-3′.

Addition of MCT4 and MCT3 basolateral sorting sequences to MCT1 was performed by amplifying selected MCT4 and MCT3 sequences (primer sequences are shown in Table S3), digesting these with BamHI and AgeI, and ligating the digested PCR products into these sites of the pEGFP-N1 MCT1 construct.

Cell Culture and Transfection

MDCK and MDCK μ1B knock-down cells were cultured in Dulbecco's modified Eagle medium (DMEM) containing 4.5 g/L glucose (Cellgro), 2 mM L-glutamine, 1% penicillin/streptomycin and 5% fetal bovine serum. MDCK μ1B knock-down cells were previously made and characterized by our group (20). MDCK cells in 35 mm dishes or on 12mm Transwell (cat. 3460 for immunofluorescence; cat. 3401 for biotinylation; Corning Costar) filters were transfected with 0.4 μg plasmid DNA using Effectene transfection reagent (Qiagen) as per manufacturer's instructions and were selected for pEGFP-N1 vectors with 2 mg/ml G418 (Cellgro). MDCK cells transfected with pcDNA6 rCD147-L252A were selected with 60 μg/ml blasticidin. At least three transfections were performed for each construct to confirm consistency of polarity. One stable, but not clonally-derived cell line was generated from each set of transfections.

Antibodies

Monoclonal antibody against the ectodomain of rCD147 (RET-PE2 hybridoma) was kindly provided by Dr. Colin Barnstable. MCT4- and MCT1-specific peptide antibodies raised in rabbit were generated previously (33). It should be noted that the MCT4 antibody was raised to the C-terminus of MCT4 and therefore detects the p75-MCT4:CT and p75-MCT4:441-465 fusion proteins, but cannot detect any of the smaller constructs. Monoclonal p75 antibody ME 20.4 used was raised against the extracellular domain of human p75 (62). Secondary antibodies used for immunofluorescence were Alexa Fluor 488 or 555-tagged anti-mouse IgG and Alexa Fluor 555-tagged anti-rabbit IgG (Invitrogen). GP135 antibody was described previously (63). The Na-K ATPase antibody a5 clone developed by Fambrough, D.M. was obtained from the Developmental Studies Hybridoma Bank developed under the auspices of the NICHD and maintained by The University of Iowa.

Animals

Mice (C57BL/6) were obtained from Charles Rivers and maintained on a 12 h light:dark cycle. The animals were sacrificed during the light period of the cycle and all experiments were performed in compliance with National Institutes of Health guidelines, as approved by the Institutional Animal Care and Use Committees of the Thomas Jefferson University.

Immunofluorescence and Confocal Microscopy

Stably, but non-clonally, selected MDCK cells were plated on 12mm Transwell filters at a density of 2×10^5 cells per well and cells were allowed to polarize for at least four days after reaching confluency. Transepithelial resistance was measured to be ≥175 Ω/cm^2. Cells were washed twice with phosphate-buffered saline with calcium (1mM) and magnesium (1mM) (PBS) and fixed in 4% paraformaldehyde in PBS for 5 min at room temperature followed by 20 min at 4°C. Cells were permeabilized with methanol and blocked for 1 h with 5% BSA in phosphate buffered saline including 0.1% Tween-20 (PBS-T) before incubating overnight with primary antibodies diluted 1:500 in 1% BSA in PBS-T. Secondary antibodies were diluted 1:500 in 1% BSA in PBS-T and incubated 1 h before washing and mounting dishes with gelvatol. Immunofluorescence labeling was detected with a Zeiss LSM 510 confocal microscope (Zeiss Microscope Imaging, Inc., Thornwood, NY). All images were acquired using a 63× objective with a 2× zoom at 1024×1024 resolution. Images were exported as raw TIF files using LSM Image Browser software (Version 4.2.0.121, Carl Zeiss GmbH Jena 1997-2006; Zeiss Microscope Imaging, Inc., Thornwood, NY). Adjustments were made to brightness and contrast only. MDCK cells are shown as X-Y projections of a 660×500 pixel region of the entire Z-stack and/or slices of X-Z cross sections. Bars in all images are 10μm. The 660×500 pixel region was chosen as a size which allowed good cell detail to be observed while also including sufficient cells for data to be representative. At least two

images were acquired for each filter. For colocalization analysis, the Z-stacks were opened in Macbiophotonics ImageJ, the red and green channels were split, background areas were subtracted with a standard deviation of 2.0 for each channel, and a 75 iteration colocalization test was performed with Fay randomization on a defined region of interest from each channel that encompassed at least four cells. A colocalization test was performed between the red and green channels to determine a Pearson's colocalization coefficient. Two regions of interest were defined and analyzed for each Z-stack and at least two Z-stacks were analyzed for each construct.

For tissue sections, mice were euthanized by overdose of anesthetic, after cardiac perfusion with 4% Paraformaldehyde in PBS. Tissues were removed, washed in PBS and cryoprotected by with 30% sucrose/PBS prior to embedding in O.C.T. Compound (Tissue-Tek). Cryosections (8-10 μm) were cut and collected on Superfrost glass slides (Fisher Scientific, Inc.). Sections were rehydrated then blocked and labeled with antibodies as described above. Sections were analyzed with a Zeiss Laser Scanning LSM 510 (Zeiss Microscope imaging, Inc. Thornwood, NY).

siRNA transfection

MDCK cells were transfected with CHC siRNA consisting of two siRNA duplexes (5′-UAAUCCAAUUCGAAGACCAAU-3′ and 5′-GUAUGAUGCUGCUAAACUA-3′, characterized previously (16) using a Neon electroporator (Invitrogen). Briefly, cells were trypsinized, washed twice in PBS and resuspended in Resuspension Buffer (Invitrogen) to achieve 3×10^5 cells and 0.5μl 10μM siRNA per 10μl transfection. Cells were pulsed three times at 1300 V for 10 ms each. Cells were plated on 12mm Transwell filters and biotinylated or fixed 72 h following transfection. Transepithelial resistance was measured to be ≥175 Ω/cm^2 in all transfected cells at this time.

Cell-surface biotinylation

MDCK cells cultured and polarized on 12mm Transwell filters as described above, were washed twice with PBS and incubated at 4°C for 20 min with 0.5 mg/ml EZ-link Sulfo-NHS Biotin (Thermo Scientific) diluted in PBS in either the top or bottom chamber. The reaction was quenched by washing the cells three times with PBS containing 100 mM glycine. Protein was extracted with Triton lysis buffer [25 mmol/l HEPES (pH 7.4), 150 mmol/l NaCl, 5 mmol/l MgCl, 1% Triton X-100 detergent] containing protease inhibitors (Sigma) and labeled proteins from 150 μg of cell lysates were precipitated with streptavidin-agarose beads (Thermo Scientific) for four hours rotating at 4°C. Beads were washed three times with Triton lysis buffer, and eluted with 50 μl 2× LDS sample buffer (Invitrogen).

Supplementary Material

Refer to Web version on PubMed Central for supplementary material.

Acknowledgments

This work was supported by NIH grants EY-012042 to NJP and EY08538 and GM34107 to ERB. JJC was supported by an NIH post-doctoral training grant (P32-ES-07282).

References

1. Brown D, Stow JL. Protein trafficking and polarity in kidney epithelium: from cell biology to physiology. Physiol Rev. 1996; 76(1):245–297. [PubMed: 8592730]
2. Philp, NJ.; Shoshani, L.; Cereijido, M.; Rodriguez-Boulan, E. Epithelial Domains. In: Nabi, IR., editor. Cellular Domains. Wiley Press; 2010.

3. Gonzalez A, Rodriguez-Boulan E. Clathrin and AP1B: key roles in basolateral trafficking through trans-endosomal routes. FEBS Lett. 2009; 583(23):3784–3795. [PubMed: 19854182]
4. Weisz OA, Rodriguez-Boulan E. Apical trafficking in epithelial cells: signals, clusters and motors. JCell Sci. 2009; 122(Pt 23):4253–4266. [PubMed: 19923269]
5. Mellman I, Nelson WJ. Coordinated protein sorting, targeting and distribution in polarized cells. NatRevMolCell Biol. 2008; 9(11):833–845.
6. Matter K, Yamamoto EM, Mellman I. Structural requirements and sequence motifs for polarized sorting and endocytosis of LDL and Fc receptors in MDCK cells. JCell Biol. 1994; 126(4):991–1004. [PubMed: 8051216]
7. Thomas DC, Brewer CB, Roth MG. Vesicular stomatitis virus glycoprotein contains a dominant cytoplasmic basolateral sorting signal critically dependent upon a tyrosine. JBiolChem. 1993; 268(5):3313–3320.
8. Dargemont C, Le Bivic A, Rothenberger S, Iacopetta B, Kuhn LC. The internalization signal and the phosphorylation site of transferrin receptor are distinct from the main basolateral sorting information. EMBO J. 1993; 12(4):1713–1721. [PubMed: 8467813]
9. Odorizzi G, Trowbridge IS. Structural requirements for basolateral sorting of the human transferrin receptor in the biosynthetic and endocytic pathways of Madin-Darby canine kidney cells. JCell Biol. 1997; 137(6):1255–1264. [PubMed: 9182660]
10. Reich V, Mostov K, Aroeti B. The basolateral sorting signal of the polymeric immunoglobulin receptor contains two functional domains. JCell Sci. 1996; 109(Pt 8):2133–2139. [PubMed: 8856509]
11. Deora AA, Gravotta D, Kreitzer G, Hu J, Bok D, Rodriguez-Boulan E. The basolateral targeting signal of CD147 (EMMPRIN) consists of a single leucine and is not recognized by retinal pigment epithelium. MolBiolCell. 2004; 15(9):4148–4165.
12. Wehrle-Haller B, Imhof BA. Stem cell factor presentation to c-Kit. Identification of a basolateral targeting domain. JBiolChem. 2001; 276(16):12667–12674.
13. Iverson HA, Fox D III, Nadler LS, Klevit RE, Nathanson NM. Identification and structural determination of the M(3) muscarinic acetylcholine receptor basolateral sorting signal. JBiolChem. 2005; 280(26):24568–24575.
14. He C, Hobert M, Friend L, Carlin C. The epidermal growth factor receptor juxtamembrane domain has multiple basolateral PM localization determinants, including a dominant signal with a polyproline core. JBiolChem. 2002; 277(41):38284–38293.
15. Maday S, Anderson E, Chang HC, Shorter J, Satoh A, Sfakianos J, Folsch H, Anderson JM, Walther Z, Mellman I. A PDZ-binding motif controls basolateral targeting of syndecan-1 along the biosynthetic pathway in polarized epithelial cells. Traffic. 2008; 9(11):1915–1924. [PubMed: 18764819]
16. Deborde S, Perret E, Gravotta D, Deora A, Salvarezza S, Schreiner R, Rodriguez-Boulan E. Clathrin is a key regulator of basolateral polarity. Nature. 2008; 452(7188):719–723. [PubMed: 18401403]
17. Bonifacino JS, Traub LM. Signals for sorting of transmembrane proteins to endosomes and lysosomes. AnnuRevBiochem. 2003; 72:395–447.
18. Folsch H, Ohno H, Bonifacino JS, Mellman I. A novel clathrin adaptor complex mediates basolateral targeting in polarized epithelial cells. Cell. 1999; 99(2):189–198. [PubMed: 10535737]
19. Gan Y, McGraw TE, Rodriguez-Boulan E. The epithelial-specific adaptor AP1B mediates post-endocytic recycling to the basolateral membrane. NatCell Biol. 2002; 4(8):605–609.
20. Gravotta D, Deora A, Perret E, Oyanadel C, Soza A, Schreiner R, Gonzalez A, Rodriguez-Boulan E. AP1B sorts basolateral proteins in recycling and biosynthetic routes of MDCK cells. ProcNatlAcadSciUSA. 2007; 104(5):1564–1569.
21. Cancino J, Torrealba C, Soza A, Yuseff MI, Gravotta D, Henklein P, Rodriguez-Boulan E, Gonzalez A. Antibody to AP1B adaptor blocks biosynthetic and recycling routes of basolateral proteins at recycling endosomes. MolBiolCell. 2007; 18(12):4872–4884.
22. Diaz F, Gravotta D, Deora A, Schreiner R, Schoggins J, Falck-Pedersen E, Rodriguez-Boulan E. Clathrin adaptor AP1B controls adenovirus infectivity of epithelial cells. ProcNatlAcadSciUSA. 2009; 106(27):11143–11148.

23. Schreiner R, Frindt G, Diaz F, Carvajal-Gonzalez JM, Bay AE Perez, Palmer LG, Marshansky V, Brown D, Philp NJ, Rodriguez-Boulan E. The absence of a clathrin adapter confers unique polarity essential to proximal tubule function. Kidney Int. 2010; 78(4):382–388. [PubMed: 20531453]
24. Broer S. Apical transporters for neutral amino acids: physiology and pathophysiology. Physiology(Bethesda). 2008; 23:95–103. [PubMed: 18400692]
25. Halestrap AP, Meredith D. The SLC16 gene family-from monocarboxylate transporters (MCTs) to aromatic amino acid transporters and beyond. Pflugers Arch. 2004; 447(5):619–628. [PubMed: 12739169]
26. Meredith D, Christian HC. The SLC16 monocaboxylate transporter family. Xenobiotica. 2008; 38(7-8):1072–1106. [PubMed: 18668440]
27. Wilson MC, Jackson VN, Heddle C, Price NT, Pilegaard H, Juel C, Bonen A, Montgomery I, Hutter OF, Halestrap AP. Lactic acid efflux from white skeletal muscle is catalyzed by the monocarboxylate transporter isoform MCT3. JBiolChem. 1998; 273(26):15920–15926.
28. Dimmer KS, Friedrich B, Lang F, Deitmer JW, Broer S. The low-affinity monocarboxylate transporter MCT4 is adapted to the export of lactate in highly glycolytic cells. BiochemJ. 2000; 350(Pt 1):219–227. [PubMed: 10926847]
29. Bonen A, Miskovic D, Tonouchi M, Lemieux K, Wilson MC, Marette A, Halestrap AP. Abundance and subcellular distribution of MCT1 and MCT4 in heart and fast-twitch skeletal muscles. AmJPhysiol EndocrinolMetab. 2000; 278(6):E1067–E1077.
30. Daniele LL, Sauer B, Gallagher SM, Pugh EN Jr. Philp NJ. Altered visual function in monocarboxylate transporter 3 (Slc16a8) knockout mice. AmJPhysiol Cell Physiol. 2008; 295(2):C451–C457.
31. Philp NJ, Yoon H, Grollman EF. Monocarboxylate transporter MCT1 is located in the apical membrane and MCT3 in the basal membrane of rat RPE. AmJPhysiol. 1998; 274(6 Pt 2):R1824–R1828.
32. Deora AA, Philp N, Hu J, Bok D, Rodriguez-Boulan E. Mechanisms regulating tissues-pecific polarity of monocarboxylate transporters and their chaperone CD147 in kidney and retinal epithelia. ProcNatlAcadSciUSA. 2005; 102(45):16245–16250.
33. Philp NJ, Wang D, Yoon H, Hjelmeland LM. Polarized expression of monocarboxylate transporters in human retinal pigment epithelium and ARPE-19 cells. Invest OphthalmolVisSci. 2003; 44(4):1716–1721.
34. Gallagher SM, Castorino JJ, Wang D, Philp NJ. Monocarboxylate transporter 4 regulates maturation and trafficking of CD147 to the PM in the metastatic breast cancer cell line MDA-MB-231. Cancer Res. 2007; 67(9):4182–4189. [PubMed: 17483329]
35. Garcia CK, Brown MS, Pathak RK, Goldstein JL. cDNA cloning of MCT2, a second monocarboxylate transporter expressed in different cells than MCT1. JBiolChem. 1995; 270(4): 1843–1849.
36. Koho N, Maijala V, Norberg H, Nieminen M, Poso AR. Expression of MCT1, MCT2 and MCT4 in the rumen, small intestine and liver of reindeer (Rangifer tarandus tarandus L.). Comp BiochemPhysiol A MolIntegrPhysiol. 2005; 141(1):29–34.
37. Nakai M, Chen L, Nowak RA. Tissue distribution of basigin and monocarboxylate transporter 1 in the adult male mouse: a study using the wild-type and basigin gene knockout mice. AnatRecA DiscovMolCell EvolBiol. 2006; 288(5):527–535.
38. Fanelli A, Grollman EF, Wang D, Philp NJ. MCT1 and its accessory protein CD147 are differentially regulated by TSH in rat thyroid cells. AmJPhysiol EndocrinolMetab. 2003; 285(6):E1223–E1229.
39. Gill RK, Saksena S, Alrefai WA, Sarwar Z, Goldstein JL, Carroll RE, Ramaswamy K, Dudeja PK. Expression and membrane localization of MCT isoforms along the length of the human intestine. AmJPhysiol Cell Physiol. 2005; 289(4):C846–C852.
40. Philp NJ, Ochrietor JD, Rudoy C, Muramatsu T, Linser PJ. Loss of MCT1, MCT3, and MCT4 expression in the retinal pigment epithelium and neural retina of the 5A11/basigin-null mouse. Invest OphthalmolVisSci. 2003; 44(3):1305–1311.

41. Le Bivic A, Sambuy Y, Patzak A, Patil N, Chao M, Rodriguez-Boulan E. An internal deletion in the cytoplasmic tail reverses the apical localization of human NGF receptor in transfected MDCK cells. J Cell Biol. 1991; 115(3):607–618. [PubMed: 1655809]

42. Le Gall AH, Powell SK, Yeaman CA, Rodriguez-Boulan E. The neural cell adhesion molecule expresses a tyrosine-independent basolateral sorting signal. JBiolChem. 1997; 272(7):4559–4567.

43. Breuza L, Garcia M, Delgrossi MH, Le Bivic A. Role of the membrane-proximal O-glycosylation site in sorting of the human receptor for neurotrophins to the apical membrane of MDCK cells. ExpCell Res. 2002; 273(2):178–186.

44. Dillon C, Creer A, Kerr K, Kumin A, Dickson C. Basolateral targeting of ERBB2 is dependent on a novel bipartite juxtamembrane sorting signal but independent of the C-terminal ERBIN-binding domain. MolCell Biol. 2002; 22(18):6553–6563.

45. Lipardi C, Ruggiano G, Perrone L, Paladino S, Monlauzeur L, Nitsch L, Le Bivic A, Zurzolo C. Differential recognition of a tyrosine-dependent signal in the basolateral and endocytic pathways of thyroid epithelial cells. Endocrinology. 2002; 143(4):1291–1301. [PubMed: 11897685]

46. Sargiacomo M, Lisanti M, Graeve L, Le Bivic A, Rodriguez-Boulan E. Integral and peripheral protein composition of the apical and basolateral membrane domains in MDCK cells. J Membr Biol. 1989; 107(3):277–286. [PubMed: 2716048]

47. Munro M, Akkam Y, Curtin KD. Mutational analysis of Drosophila basigin function in the visual system. Gene. 2010; 449(1-2):50–58. [PubMed: 19782733]

48. Wilson MC, Meredith D, Bunnun C, Sessions RB, Halestrap AP. Studies on the DIDS-binding site of monocarboxylate transporter 1 suggest a homology model of the open conformation and a plausible translocation cycle. JBiolChem. 2009; 284(30):20011–20021.

49. Wild-Bode C, Fellerer K, Kugler J, Haass C, Capell A. A basolateral sorting signal directs ADAM10 to adherens junctions and is required for its function in cell migration. JBiolChem. 2006; 281(33):23824–23829.

50. Madrid R, Le Maout S, Barrault MB, Janvier K, Benichou S, Merot J. Polarized trafficking and surface expression of the AQP4 water channel are coordinated by serial and regulated interactions with different clathrin-adaptor complexes. EMBO J. 2001; 20(24):7008–7021. [PubMed: 11742978]

51. Simmen T, Nobile M, Bonifacino JS, Hunziker W. Basolateral sorting of furin in MDCK cells requires a phenylalanine-isoleucine motif together with an acidic amino acid cluster. MolCell Biol. 1999; 19(4):3136–3144.

52. Murphy SJ, Shapira KE, Henis YI, Leof EB. A unique element in the cytoplasmic tail of the type II transforming growth factor-beta receptor controls basolateral delivery. MolBiolCell. 2007; 18(10): 3788–3799.

53. Suemizu H, Radosavljevic M, Kimura M, Sadahiro S, Yoshimura S, Bahram S, Inoko H. A basolateral sorting motif in the MICA cytoplasmic tail. ProcNatlAcadSciUSA. 2002; 99(5):2971–2976.

54. Li HC, Collier JH, Shawki A, Rudra JS, Li EY, Mackenzie B, Soleimani M. Sequence- or position-specific mutations in the carboxyl-terminal FL motif of the kidney sodium bicarbonate cotransporter (NBC1) disrupt its basolateral targeting and alpha-helical structure. JMembrBiol. 2009; 228(2):111–124.

55. Wolff SC, Qi AD, Harden TK, Nicholas RA. Charged residues in the C-terminus of the P2Y1 receptor constitute a basolateral-sorting signal. JCell Sci. 2010; 123(Pt 14):2512–2520. [PubMed: 20592187]

56. Vagin O, Kraut JA, Sachs G. Role of N-glycosylation in trafficking of apical membrane proteins in epithelia. Am J Physiol Renal Physiol. 2009; 296(3):F459–469. [PubMed: 18971212]

57. Yang J, Bhaumik M, Liu Y, Stanley P. Regulation of N-linked glycosylation. Neuronal cell-specific expression of a 5′ extended transcript from the gene encoding N-acetylglucosaminyltransferase I. Glycobiology. 1994; 4(5):703–712. [PubMed: 7881185]

58. Kommareddi PK, Nair TS, Thang LV, Galano MM, Babu E, Ganapathy V, Kanazawa T, McHugh JB, Carey TE. Isoforms, expression, glycosylation, and tissue distribution of CTL2/SLC44A2. Protein J. 2010; 29(6):417–426. [PubMed: 20665236]

59. Paulson JC, Weinstein J, Schauer A. Tissue-specific expression of sialyltransferases. J Biol Chem. 1989; 264(19):10931–10934. [PubMed: 2738054]

60. O'Hanlon TP, Lau KM, Wang XC, Lau JT. Tissue-specific expression of beta-galactoside alpha-2,6-sialyltransferase. Transcript heterogeneity predicts a divergent polypeptide. J Biol Chem. 1989; 264(29):17389–17394. [PubMed: 2793863]

61. Gallagher SM, Castorino JJ, Philp NJ. Interaction of monocarboxylate transporter 4 with beta1-integrin and its role in cell migration. AmJPhysiol Cell Physiol. 2009; 296(3):C414–C421.

62. Ross AH, Grob P, Bothwell M, Elder DE, Ernst CS, Marano N, Ghrist BF, Slemp CC, Herlyn M, Atkinson B. Characterization of nerve growth factor receptor in neural crest tumors using monoclonal antibodies. ProcNatlAcadSciUSA. 1984; 81(21):6681–6685.

63. Herzlinger DA, Ojakian GK. Studies on the development and maintenance of epithelial cell surface polarity with monoclonal antibodies. J Cell Biol. 1984; 98(5):1777–1787. [PubMed: 6725399]

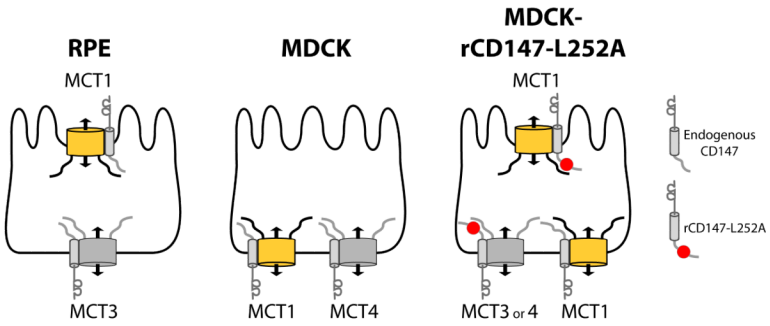

Figure 1. Models of MCT sorting in different epithelia

In RPE cells, MCT1/CD147 is polarized to the apical and MCT3/CD147 to the basolateral membrane. In wild-type MDCK cells, all MCT/CD147 complexes are sorted basolaterally. When rCD147-L252A is expressed in MDCK cells, MCT1/ rCD147-L252A complexes are localized to the apical membrane while MCT1/CD147 complexes are basolateral. In contrast, endogenously expressed MCT4 or exogenously expressed MCT3 remain basolateral whether they are complexed with endogenous CD147 or with exogenously expressed rCD147-L252A, indicating that MCT3 and MCT4 both harbor BLSS.

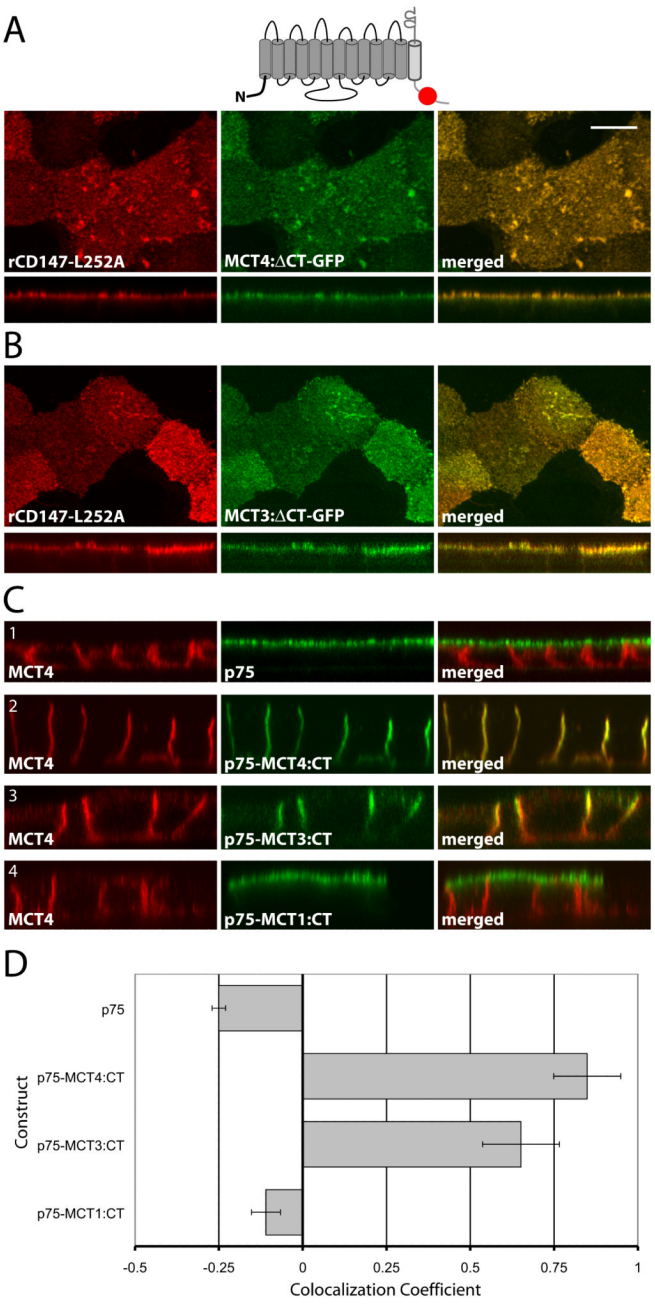

Figure 2. The MCT3 and MCT4 C-terminal cytoplasmic tails dictate polarity

Vectors expressing C-terminally truncated **(A)** MCT4-GFP and **(B)** MCT3-GFP fusions were stably expressed MDCK-rCD147-L252A cells. Cells were cultured on Transwell inserts and four days after they reached confluency, were fixed and immunolabeled with anti-rat CD147 antibody (red). Images of the MDCK cells were acquired using LSCM. Upper panels of each row are X-Y images of projections of the entire Z-stack. Bottom panels of each row are X-Z sections from the Z-stack. **(C)** MDCK cells were transfected with vectors expressing p75 with no cytoplasmic tail or with the appended MCT4, MCT3 or MCT1 C-terminal tails. Polarized MDCK cells stably expressing the fusion proteins were fixed and immunolabeled with p75 antibody (green) to detect the p75-MCT chimeras and

MCT4 antibody (red) to detect endogenous MCT4 as basolateral marker. Images are shown as X-Y images of projections of the entire Z-stack (upper panels in each row) and X-Z sections of the Z-stack (bottom panels in each row). Bar=10μm, all images are same scale. **(D)** Colocalization analysis was performed on the red versus green channels of confocal Z-stacks as described in *Methods* and Pearson's correlation coefficients were plotted. Error bars are standard deviations of the colocalization coefficients from at least four regions of interest.

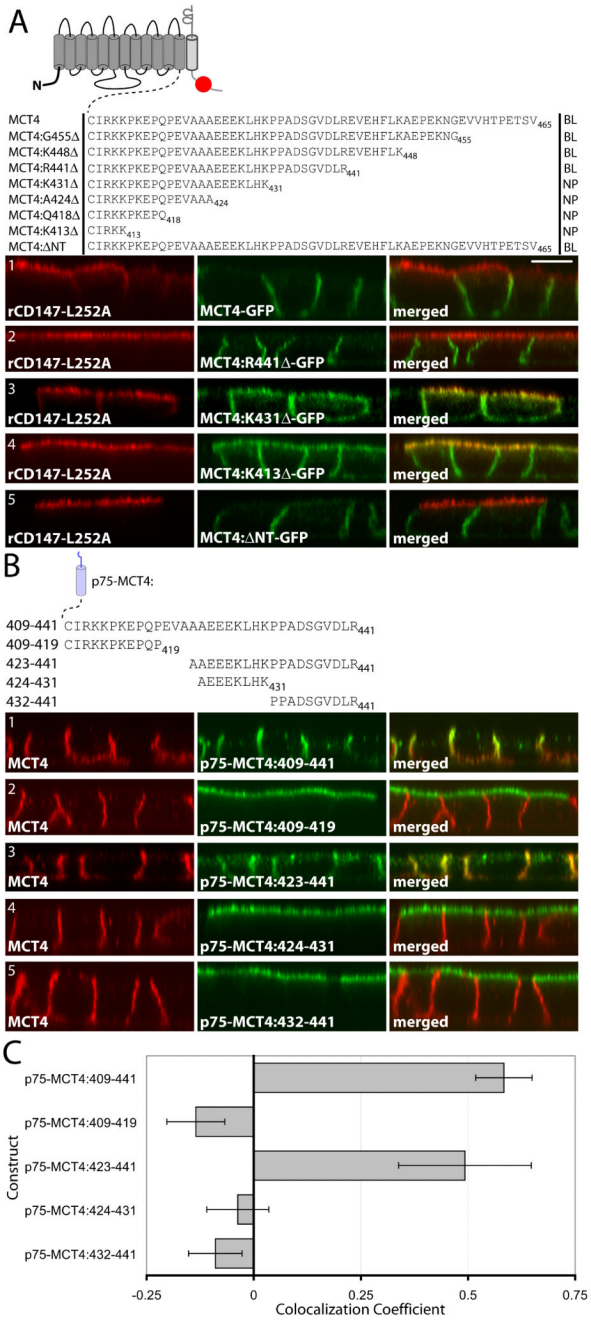

Figure 3. Identification of the MCT4 BLSS

(A) In order to identify the general location of the BLSS, additional constructs with progressive C-terminal truncations of MCT4 were generated as GFP fusions and stably expressed in MDCK-rCD147-L252A cells. The C-terminal tail sequences and resulting polarity for each construct are shown in the table above the figure (NP=nonpolar, BL=basolateral). Polarized cells cultured on Transwell inserts were fixed and immunolabeled with anti-rat CD147 antibody (red). Images of the MDCK cells were acquired using LSCM. **(B)** An array of p75 fusion constructs was generated to identify the BLSS activity within MCT4 amino acids 409-441. Polarized MDCK cells stably expressing the p75 fusion constructs were fixed and immunolabeled with an anti-p75 antibody (green)

to detect the transgenes and anti-MCT4 antibody (red) as an endogenous basolateral marker. Confocal images are shown as X-Z images of representative sections of the Z-stack. Bar=10μm, all images are same scale. **(C)** Colocalization analysis was performed on the red versus green channels of confocal Z-stacks as described in *Methods* and Pearson's colocalization coefficients were plotted. Error bars are standard deviations of the colocalization coefficients from at least four regions of interest.

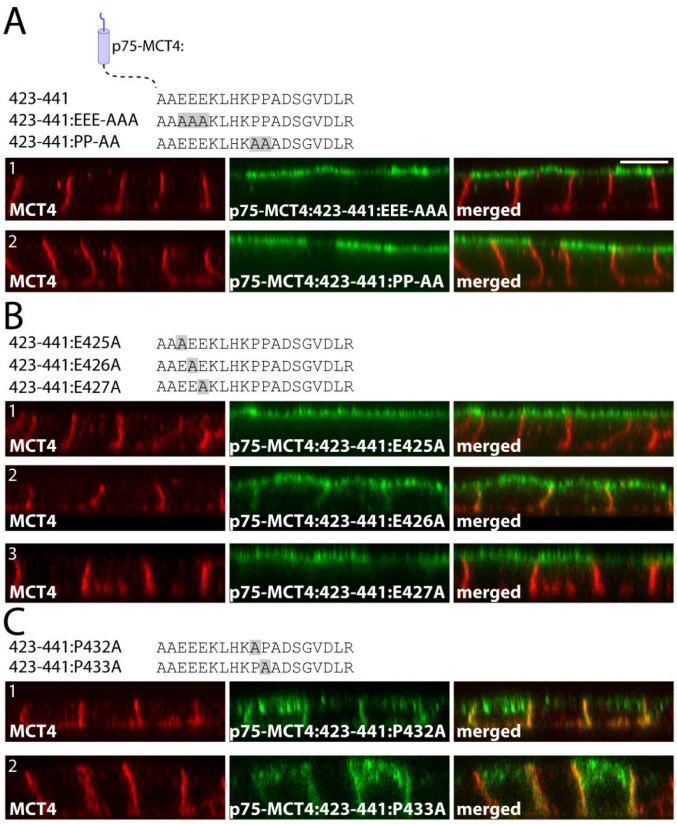

Figure 4. Critical roles of EEE and PP within the MCT4:423-441 BLSS

(A) Polarized MDCK cells stably expressing p75-MCT4:423-441 with either all E425, E426, E427 or both P432 and P433 residues mutated to alanine were fixed and immunolabeled with anti-p75 antibody (green) to detect the transgenes and anti-MCT4 antibody (red) as an endogenous basolateral marker. The C-terminal tail sequences for each construct are shown above the figure. Further mutations were made to the individual **(B)** glutamate and **(C)** proline residues. Confocal images are shown as X-Z images of representative sections of the Z-stack. Bar=10μm, all images are same scale.

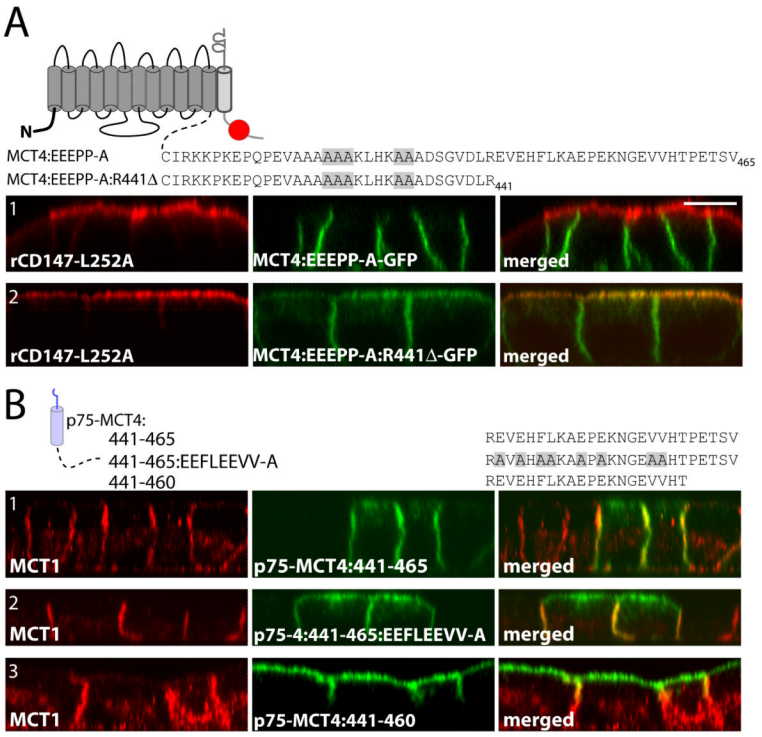

Figure 5. Identification of an additional BLSS within MCT4

(A) To confirm the BLSS activity of the glutamate and proline residues they were mutated in MCT4-GFP and MCT4:R441Δ-GFP and constructs were stably expressed in MDCK-rCD147-L252A cells. Polarized cells were fixed and immunolabeled with anti-rat CD147 antibody (red). **(B)** Polarized MDCK cells stably expressing p75-MCT4:441-465 and mutated and truncated p75-MCT4:441-465 constructs were fixed and immunolabeled with anti-p75 antibody (green) to detect the transgenes and anti-MCT4 antibody (red) to detect endogenous MCT4 (red). Confocal images are shown as X-Z images of representative sections of from the Z-stack. Bar=10μm, all images are same scale.

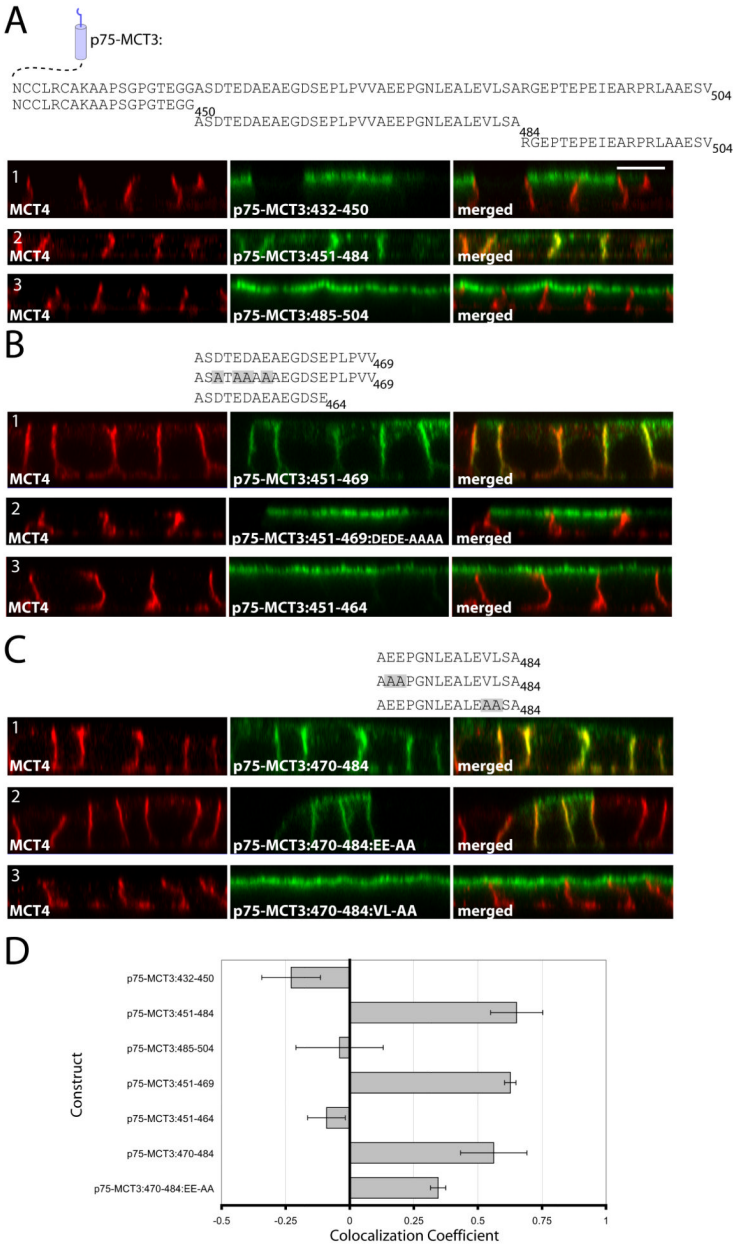

Figure 6. Identifying the BLSS of MCT3

p75-MCT3 tail constructs comprised of adjacent regions of the MCT3 C-terminal cytoplasmic tail were generated and stably expressed in MDCK cells. The C-terminal tail sequences for each construct are shown above the figure. **(A)** p75-MCT3 fusions of the C-terminal cytoplasmic tail divided into three sections. MCT3:451-484 was divided into two smaller fragments 451-469 **(B)** and 470-484 **(C)** and additional mutation analysis was performed on each of these regions. Polarized cells expressing the p75-MCT3 fusion constructs were fixed and immunolabeled with anti-p75 antibody (green) to detect the transgenes and anti-MCT4 antibody (red) to detect endogenous MCT4. Confocal images are shown as X-Z sections from the Z-stack. Bar=10μm, all images are same scale. **(D)** Colocalization analysis was performed on the red versus green channels of confocal Z-stacks as described in *Methods* and Pearson's colocalization coefficients were plotted. Error

bars are standard deviations of the colocalization coefficients from at least four regions of interest.

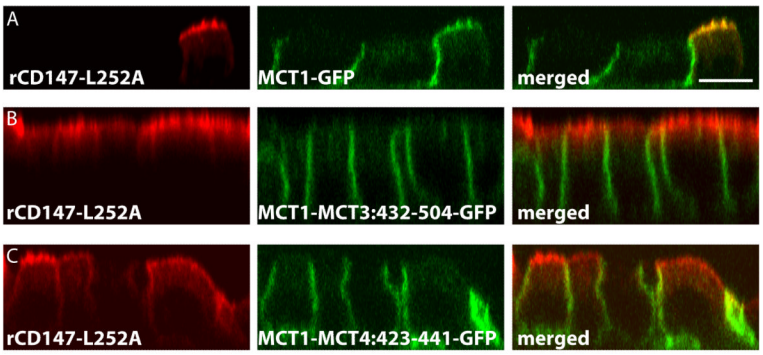

Figure 7. The BLSS of MCT3 and MCT4 are transferable to MCT1

MDCK cells stably expressing rCD147-L252A were transfected with MCT1-GFP, MCT1ΔCT-MCT3:432-504-GFP, or MCT1-MCT4:423-441-GFP constructs. Non-clonal stable cell lines were selected and cultured on Transwell inserts. Polarized cells were fixed and immunostained with anti-rCD147 antibody (red). Confocal images are shown as X-Z sections from the Z-stack. Bar=10μM, all images are same scale.

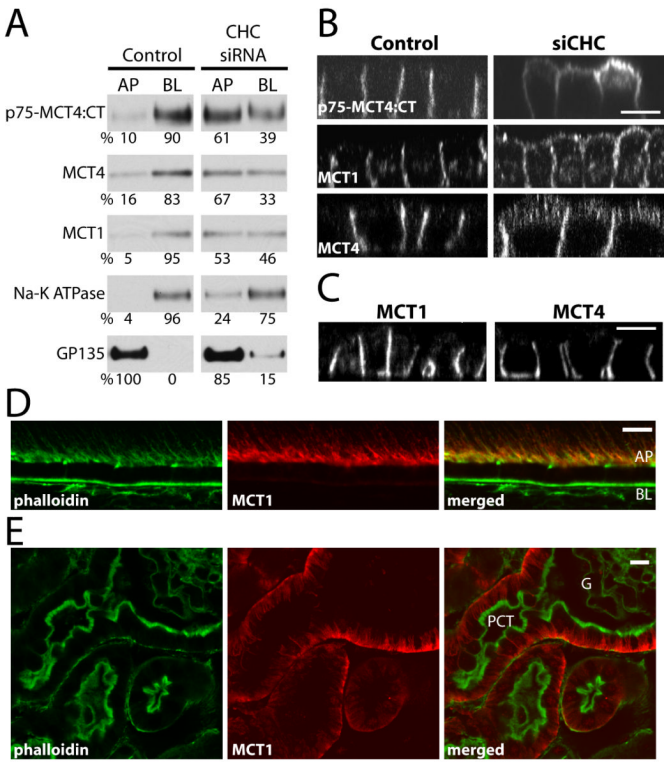

Figure 8. The steady state basolateral localization of MCTs is clathrin-dependent, but μ1B-independent

MDCK cells stably expressing p75-MCT4:CT were transfected with siRNA against CHC or luciferase (Control) and the steady-state distribution of p75-MCT4:CT and endogenously expressed proteins was determined by domain-selective cell-surface biotinylation of polarized MDCK cells cultured on Transwell inserts and western blot **(A)** and LSCM **(B)**. **(C)** Additionally, the polarity of endogenous MCT1 and MCT4 were determined by LSCM in cells where AP1B complex component μ1B was stably knocked down (20). Confocal images are shown as X-Z sections from the Z-stack. Mouse tissues sections were stained for MCT1 (red) and phalloidin (green) to show that even though neither the RPE **(D)** nor proximal convoluted tubule **(E)** express AP1B, the polarity of MCT1 is different between these tissues. AP=apical, BL=basolateral, PCT=proximal convoluted tubule; bar=10μm.

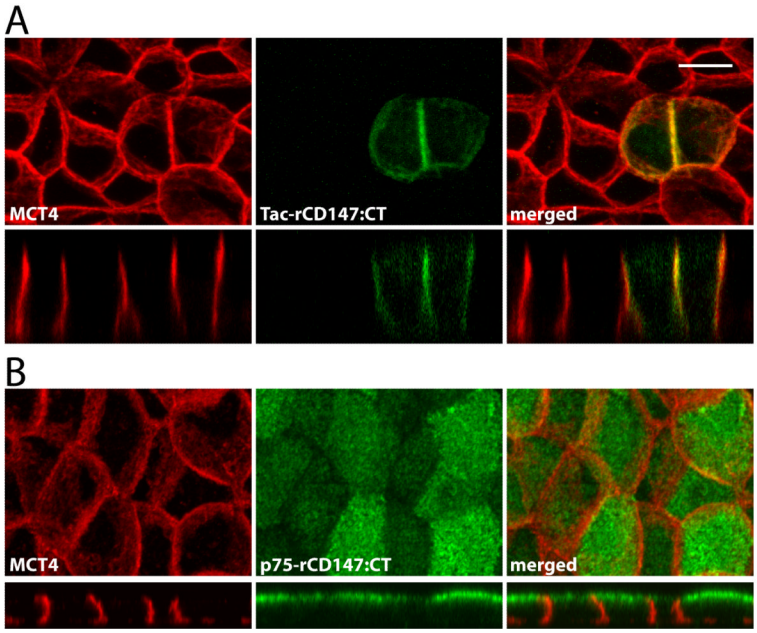

Figure 9. p75-rCD147:CT is polarized to the apical membrane in MDCK cells

(A) As previously shown, a GFP fusion protein consisting of the extracellular and transmembrane domains of Tac with the cytoplasmic domain of rCD147 was sorted basolaterally. **(B)** A p75-rCD147 fusion protein comprised of the extracellular and transmembrane domain of p75 and the cytoplasmic tail of CD147 and stably expressed in MDCK cells. Polarized MDCK-p75-rCD147 cells cultured on transwell inserts were fixed and immunolabeled with anti-p75 antibody (green) to detect the p75-CD147 fusion protein and anti-MCT4 antibody (red) as a basolateral marker. Confocal images are shown as projections of the entire Z-stack (upper panels) and X-Z images (lower panels) of representative sections of the Z-stack. Bar=10μm, all images are same scale.